

Energetics impact from the use of flexible and adaptable stiffness wheels on lunar and planetary rovers

Vassilios Papantoniou⁽¹⁾, Stylianos Skevakis⁽¹⁾, Anastasios G. Katelouzos⁽¹⁾, Ares Papantoniou⁽¹⁾, Konstantinos Kapellos⁽²⁾, Evangelos Papadopoulos⁽³⁾, Michel Van Winnendael⁽⁴⁾.

⁽¹⁾HTR ABEE, L. Kifissias 188, 14562 Athens Hellas. Email: info@htr.gr

⁽²⁾TRASYS International EEIG Interleuvenlaan 10, 3001 Heverlee Belgium. Email: Konstantinos.Kapellos@trasysinternational.com

⁽³⁾NTUA, 9 Iroon Polytechniou, 15780 Athens, Hellas. Email: egpapado@central.ntua.gr

⁽⁴⁾ESA Email: Michel.van.Winnendael@esa.int

1. Abstract

An innovative concept is presented of variable stiffness wheels, which can continuously and automatically adjust their stiffness according to soil conditions. Wheel breadboard models have been tested individually and as a set of six of them, mounted on an ExoMars-like triple bogie full-scale rover locomotion subsystem model, on a dedicated HTR-designed testbed facility. Energetics have been derived as a function of wheel stiffness, wheel load, drawbar pull and soil conditions, demonstrating a significant impact from the use of variable stiffness wheels in varying soil conditions. A wheel with low stiffness appears to need up to 30% higher net power compared to the needs of a rigid wheel for motion over *non-deformable* soils. On the other hand, an important increase of power needs is observed for stiff wheels over *deformable* soils, demonstrating the need for wheel stiffness adaptation. To this end, prototype wheels were developed consisting of metallic parts and intended for use on Lunar or Martian rovers. A specially designed mechanism permits the modification of the overall stiffness of the wheel when in contact with the soil. The test results have been organized in a comprehensive database and also are introduced in the TRASYS 3DROCS rover operations planning platform to predict the traction performance and the energetics of robotic rover vehicles, operating on Lunar or Martian soil conditions, for a speed range from 50 to 500 m/h. The results presented in this paper refer to test campaigns that took place in the context of the ESA project Adaptable Wheels for Exploration (AWE), while the experiments were conducted at HTR's Laboratories (Lamia, Greece). The related work (ESA Contract number 4000112936 /14/NL/SFE), has been performed by HTR SA Greece in collaboration with the School of Mechanical Engineering and the Control Systems Laboratory (CSL) of the National Technical University of Athens (NTUA), as well as with TRASYS International SA Belgium.

2. Introduction

Motion on soft soil with rigid or relatively stiff wheels results to considerable losses due to soil compacting and bulldozing effects. If a more flexible wheel is used, the bulldozing forces decrease, compare Fig. 1a and Fig. 1b,

where $f < F$). For a flexible wheel however, losses increase on harder soils, Fig. 1c. It appears therefore that for a given soil condition, there should exist a degree of flexibility that provides minimal losses and optimal efficiency of the wheel system. The AWE project addressed the process to be followed in defining this optimal flexibility and the experimental methodology needed to measure the benefits of the application of the optimal flexibility in wheel energetics.

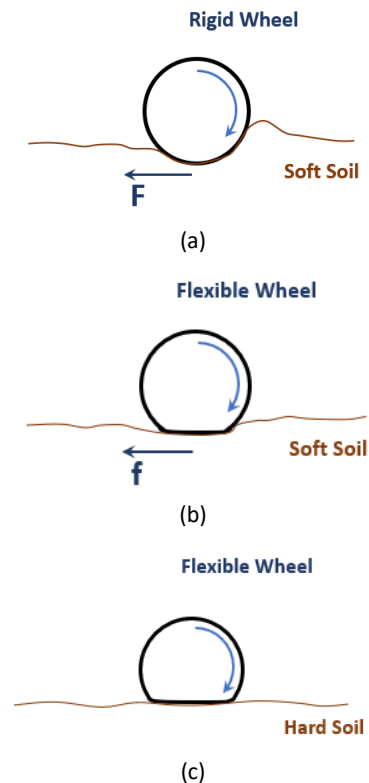


Figure 1: Effect of soil type on wheel type. (a) Rigid wheel on soft soil, (b) flexible wheel on soft soil, (c) flexible wheel on hard soil.

Clearly, the overall locomotion efficiency depends also on the actuation system used. If the wheel stiffness is optimized, while the driving actuator is operated far from its highest efficiency operational point, then the overall efficiency of the locomotion system remains sub-optimal.

In this paper, we address the issue of the optimization of a locomotion system with a given actuator, operating on a variable stiffness wheel. If an actuator has been selected for a specific mission scenario, the total benefit from the use of variable flexibility wheels also depends on the distance covered during a mission and on the variability of the soil to be traversed. Depending also on the overall mass, it can be seen that in some cases significant gains in the energetics can be obtained justifying the use of variable flexibility wheels.

As a result of the large number of experiments executed, a significant number of performance results has been obtained, regarding:

- The traction (drawbar pull versus axis load) performance of a wheel with varying stiffness on 3 types of relative density of basaltic sand soil, for various axis loads and slip ratios, characterising the tractive performance as a function of wheel stiffness, axis load, slip ratio and type of soil.
- The power needed to move a loaded wheel of variable stiffness, on 3 types of relative density basaltic sand soil, with variable speed, characterising the impact of variable stiffness, axis load, speed and soil type on the Cost of Transport [22].
- The power needed to move a loaded wheel of variable stiffness, on 3 types of relative density basaltic sand soil, with an imposed traction (Drawbar pull), as well as variable slip ratio, characterising the Power Number of the wheel / actuator system as a function of axis load, drawbar pull, slip ratio and speed [23].

The test results are presented in the following sections.

3. Test results regarding tractive performance

The wheel stiffness variation mechanism developed and integrated within the AWE project enables the modification of stiffness of the wheel in the elasticity range of $k_{min}=2500$ N/m to $k_{max}= 10000$ N/m, or a factor of 4x stiffness modification. The wheel has therefore the capability to modify its radial stiffness by a factor of 4.

During the campaign, see Fig. 2, tests were conducted with stiffness varying from 20% of the range, or 4000 N/m, to 80% of the range, or 8500 N/m. Single wheel tests focusing on tractive performance, examining the soil-wheel interaction, focused on the capacity of the wheel to generate traction as a function of soil type, soil relative density, wheel stiffness and wheel axial load.

The test procedure involved a testbed with the capacity to measure and register all critical parameters for each experiment. The testbed operates by imposing a fixed draw bar pull on the wheel or rover. This process represents a more precise way to evaluate traction performance [21]. The test process is presented schematically in Fig. 3. The motion is produced by the actuator of the wheel or rover only; no other active (motorized) elements are present on the testbed.



Figure 2: Wheel breadboards testing at HTR Laboratories on single wheel (top) and subsystem level testbeds (middle and bottom) using crushed basalt as soil.

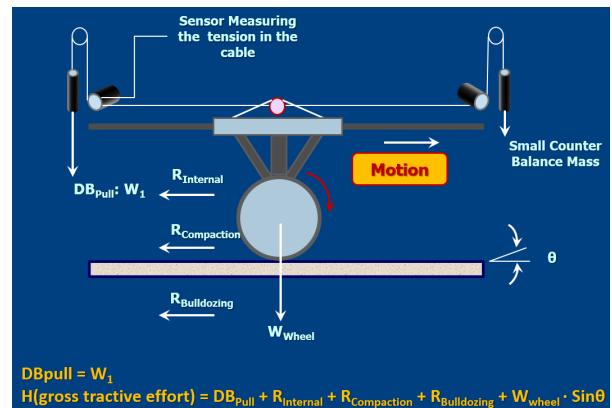


Figure 3: Net drive power in function of axis load, for minimum and maximum wheel stiffness.

The drawbar force (DB) is imposed by counterweight W_1 and is measured in real time by a dedicated force sensor. The resulting wheel motion, slippage ratio and sinkage are measured and recorded. When the DB imposed is very high, the wheel is unable to move and remains on the same position, digging into the sand. In many cases, under a high imposed DB, the wheel started moving with a high slip ratio, but after some distance it has been immobilised and started digging into the sand.

For such tests, the slip ratio considered has been the average observed during the duration of the entire experiment (typically 60 s).

Using this testbed, we conducted thousands of tests using single wheels or the entire 6 wheel rover. Tests addressed the variation of DB / axis load, as a function of soil conditions, slip ratio and wheel flexibility. Fig. 4 presents results from a substantial number of tests, using AWE wheels on Relative Density (ReD) 60% basaltic sand soil, for wheel stiffness of 20% and 80% of the maximum available stiffness of the AWE wheel. It can be seen that the average tractive performance (DB / Axis Load) of the wheel of 8.5 kN/m (higher stiffness), at 30% slip ratio, is better on this hard soil (average 0.6 for the stiffer wheel versus 0.52 for the wheel with the 4kN/m lower stiffness).

In Fig. 5, the same range of tests has been conducted with a basaltic sand soil of ReD 40%. In this case, the wheel with the lower stiffness (4 kN/m) performs better, (DB / Axis Load of low stiffness wheel for 30% slip ratio is 0.58, while for high (8.5 kN/m) stiffness wheel it drops to 0.50).

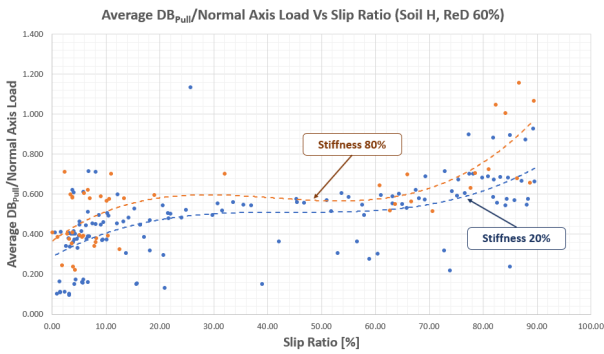


Figure 4: DB/axis load for tests on basaltic sand, ReD 60%, with stiffness varying 80 % to 20% of the maximum available stiffness of the AWE wheel.

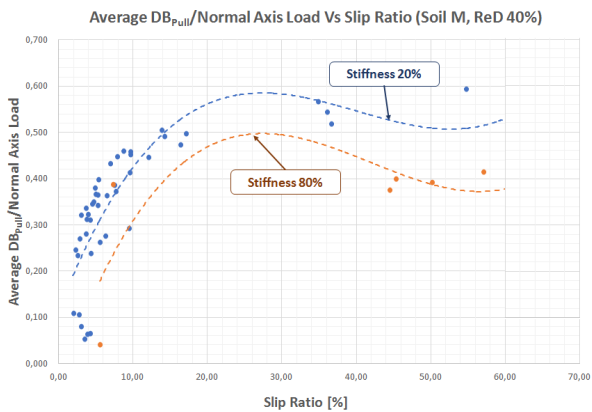


Figure 5: DB/axis load for tests on basaltic sand, ReD 40%, with stiffness varying 80 % to 20% of the maximum available stiffness of the AWE wheel.

Finally, for a soil with ReD 20%, the impact of wheel stiffness is again verified, see Fig.6. Again, a wheel of low stiffness, (4 kN/m) performs with a 0.52 DB/Axis Load at 30% slip ratio on basaltic sand 20% ReD, where a higher stiffness (8.5 kN/m) wheel produces 0.44 DB/Axis load only.

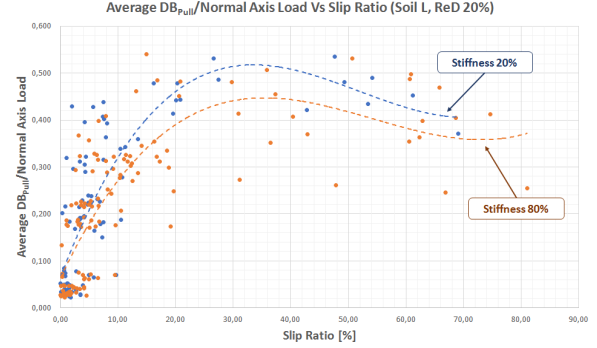


Figure 6: DB/axis load for tests on basaltic sand, ReD 20%, with stiffness varying 80 % to 20% of the maximum available stiffness of the AWE wheel.

In conclusion, it appears that a stiffer wheel performs less in terms of traction and also tends to dig in and stall, when the relative density of the soil decreases and the imposed drawbar increases. The tests have been performed at a speed of 100 m/h. The results present the variation of the DB / Axis load rate as a function of slip ratio applied on the wheel during its motion on the soil. It is worth noting that in the case of basaltic soil with a ReD of 40% or lower, higher wheel flexibility favours the development of higher traction. Another observation made through these experiments is the fact that high slip ratios do not increase tractive performance when the soil is soft. A high slip ratio in this case generates a higher sinkage of the wheel, decreasing traction and possibly resulting to the wheel being completely stuck. From an efficiency and safety point of view, it appears that slip ratios up to 30% should be applied. Other reports come to similar conclusions [17].

4. Test results regarding cost of transport

A large number of tests have been conducted in HTR's facilities in order to determine the impact on energetics that can be achieved from the stiffness modification of the wheels. As a metric for efficiency, the Cost of Transport has been used. The term has been introduced by Gabrielli and Von Karman [22] and relates to:

$$\varepsilon = \frac{\text{Watt} \cdot \text{sec}}{\text{weight} \cdot \text{distance}} \quad (1)$$

where "Watt" is the power provided to the vehicle, "sec" is the duration of the motion in seconds, "weight" is the weight of the vehicle in N and "distance" is the distance covered in m. For a given vehicle, operating on a specific type of soil, the cost of transport represents a metric of its

efficiency. The cost of transport applies to all transport means, i.e. land vehicles, trains, ships, airplanes, etc. In the context of AWE, we investigated if it was possible to optimize the cost of transport for the given wheel and actuator design, by modifying the wheel stiffness and its speed. To this end, we tested a fully rigidified version of the AWE wheel, a wheel with 60% of the max stiffness that can be applied (7 kN/m) and a wheel with 20% of the max stiffness (4 kN/m) that can be applied on the wheel, on the same 40% ReD basaltic sand.

Direct measurements of the power provided to the wheel motor (without the use of the power control electronics) have been used to guarantee that the power measured was only used by the wheel motor and not by other passive components.

Tests comprised individual wheel tests as well as tests at rover level. The tests focused on the net power used by the wheel for operation on soils of various relative densities, as a function of wheel stiffness, axial load and wheel speed, affecting the resulting cost of transport of the vehicle.

Representative results can be seen in Fig. 7. The two lines represent the cost of transport for the wheel actuator for operation at a speed from 200 m/h to 500 m/h, on the same soil conditions (basaltic sand, 40% ReD). The AWE wheel, with zero draw bar and *full rigidity*, has an average cost of 0.72 with axis load of 90 N and an average cost of 0.52 with an axis load of 130 N, for the entire speed range.

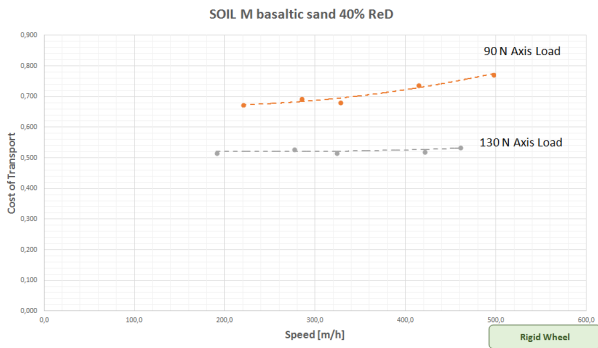


Figure 6: Cost of transport for rigid wheel with speed from 200 to 500 m/h.

The same wheel on the same soil, with a stiffness of 20% (4 kN/m), yields a cost of transport of 0.59 for axis load 90 N at 340 m/h speed and a cost of transport of 0.45 for axis load of 130 N and 370 m/h speed, see Fig. 8. The advantage of the flexible wheel on the cost of transport is obvious; however these tests also indicate that for each wheel and actuator assembly, operation points exist that provide a minimum cost of transport in terms of speed and wheel flexibility.

Finally, a wheel with stiffness of 7 kN/m (60% of the full range) operating on 40% ReD basaltic sand, produces for axis load of 90 N and 130 N as shown in

Fig. 9. The test presents a minimum CoT of 0.66 at a speed of 240 m/h for 90 N axis load, and a CoT of 0.53 at speeds ranging from 250 m/h to 480 m/h for a load of 130 N.

The obtained results show that there can be a significant impact of the wheel stiffness on the energetics of the wheel during motion with varying axis loads. Of course, if the soil conditions change, this performance can be modified (for instance, on a very soft soil, the power drain of a stiffer wheel can be expected to become higher than the drain of a more flexible wheel). Another important issue to notice here is that the results largely depend on the actuator used. Therefore, the actuator can also be optimized for minimal cost of transport.

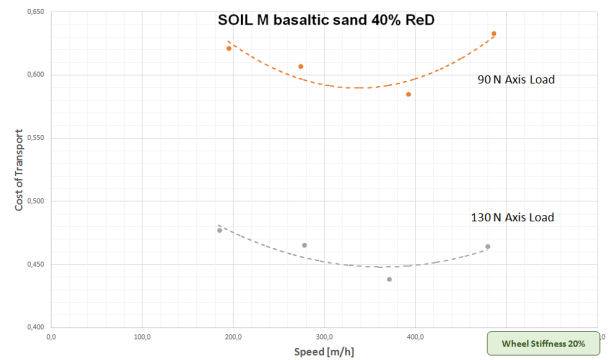


Figure 7: Cost of transport for 4 kN/m elastic wheel with speeds ranging from 150 to 500 m/h.

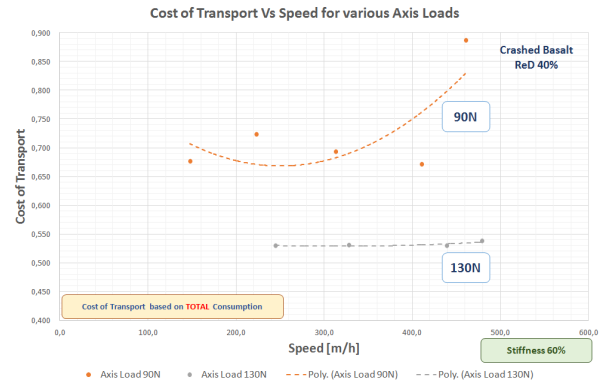


Figure 8: Cost of transport for a 7 kN/m elastic wheel with speed from 150 to 500 m/h.

5. Tests involving the Power Number

Another group of tests involves the evaluation of the wheel performance when an amount of mechanical work is “produced” (for instance, when the wheel is ascending a slope). In this case, the wheel is evaluated with the amount of energy that is provided to the wheel versus the amount of energy that is “produced” by the wheel. Then:

$$Power\ Number = \frac{Input\ Energy}{Output\ Energy} \quad (2)$$

The net power input is determined by directly measuring the electric power supplied to the wheel motor (bypassing the power control electronics), to make sure the measurement does not comprise power drain on passive elements. The duration of the test multiplied by the supplied electrical power, produces the total energy supplied. The output energy is calculated as the product of the DB developed by the wheel times the distance covered.

The tests have been performed by the AWE wheel actuator for the production of a resulting work (ascending a slope), as a function of soil conditions, axis load, imposed DB, wheel stiffness and speed. Obviously the choice of the specific actuator is a key factor, but experiments show how other factors such as wheel flexibility affect the power number and how under specific conditions the power number can be minimised (optimal configuration). Fig. 10 displays experimental results from a wheel of 7 kN/m stiffness, with 130 axis load, operating in the range of 75 to 400 m/h speed, with an imposed DB of either 40 N or 60 N. The tests took place on a 40% ReD basaltic sand. The tests produce a minimum Power Number of 4.2 in the case of 40 N DB for a speed of 400 m/h and a minimum Power Number of 3.9 for a speed of 275 m/h with a DB of 60 N.

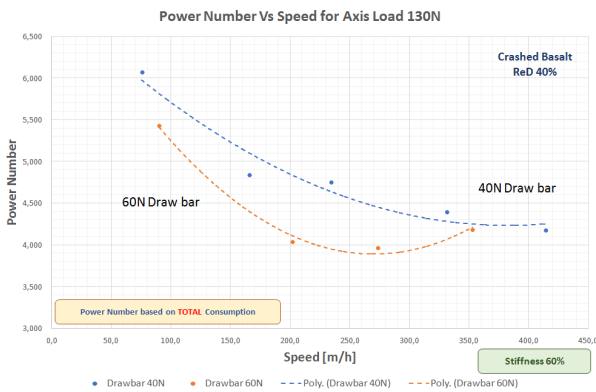


Figure 9: Power number as a function of axis load and speed for AWE actuator and wheel at 6 kN/m stiffness.

A similar set of tests is presented in Fig. 11, where the stiffness of the wheel is brought down to 4 kN/m. In this case, the experimental results show the wheel with 130N axis load, operating in the range of 100 to 400 m/h speed, with an imposed DB of 40 N or 60 N. The tests took place on 40% ReD basaltic sand. The tests produce a minimum Power Number of 4 in the case of 40 N DB for a speed of 325 m/h and a minimum Power Number of 3.6 for a speed of 300 m/h with a DB of 60 N. Therefore it appears that the stiffness decrease produced a decrease of the power number in the specific soil conditions.

The extended test campaign has produced an amount of experimental results that help answer the questions related to wheel stiffness optimization for long traverses. It appears that optimal stiffness for given soil conditions and axis load on a wheel, may significantly

modify its cost of transport for a specific speed range. This fact is important for the design of autonomous vehicles for long planetary exploration missions. This optimization process becomes more critical when the mass of the systems increases.

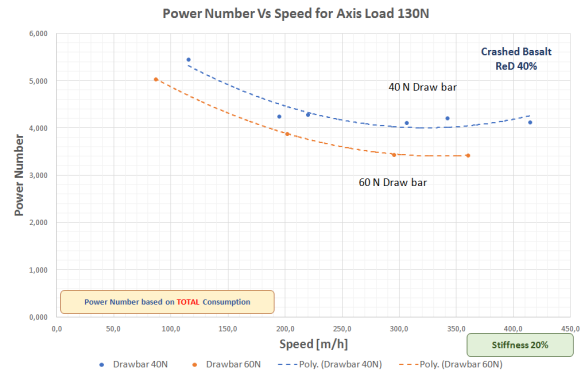


Figure 10: Power number for wheel with 4 kN/m stiffness on 40% ReD basaltic sand

6. Incorporation of test results in 3DROCS

The results of several thousands of test runs similar to those described in the previous sections have been organized by HTR and grouped in databases. To facilitate the study of rovers with different configurations of wheels, wheels of different stiffness, rovers of different design etc., and enable the appreciation of the impact of the use of these different designs on system level architecture and for different missions, the database has been introduced in the TRASYS 3DROCS rover operations planning environment, See Figs. 12-14. This enhancement of the planning environment with realistic test results, permits, to evaluate new rover and wheel design approaches during the preparation of realistic exploration mission scenarios, such as the Mars Sample Return or HERACLES mission, see Fig. 12. During real operations, the feasibility and the energy cost of a given path can be also estimated, see Fig. 13.

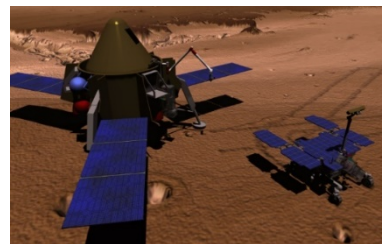


Figure 11: 3DROV Simulation Environment.



Figure 12: Typical range for SFR mission is 30 km.

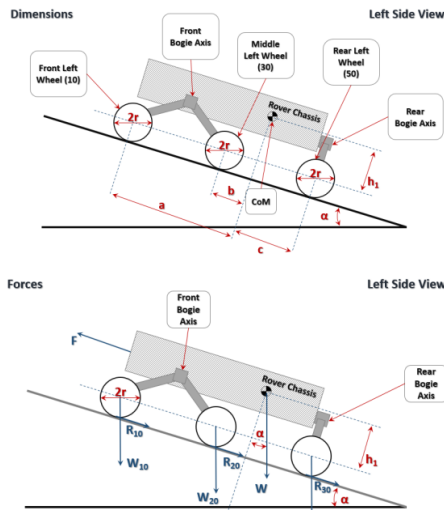


Figure 14: 3DROCS implements a rover geometry and load distribution.

For such missions, it is important from a system level point of view to optimise the actuator and wheel design of the rover in order to achieve a minimal overall cost of transport. The important parameters to optimise include:

- Cost of transport on horizontal soil conditions, as a function of: soil type, speed, axis load, wheel stiffness, wheel diameter and actuator used.
- Power number on soils with slopes, as a function of: soil type, axis load, slope inclination, speed, wheel stiffness, wheel diameter and actuator used.

To facilitate this complex optimisation problem which depends heavily on a given trajectory, a simulation – based tool that feeds from existing experimental data mined from tests on similar conditions can be useful. For example, if we assume that on the basis of experimental results, the behaviour of a certain wheel and actuator type can be statistically predicted, then for a given rover geometry Figs. 15-16, one can claim that the traction capacity and the energetics of the (specific) wheels and (specific) rover geometry, can be approximated for similar soil conditions.

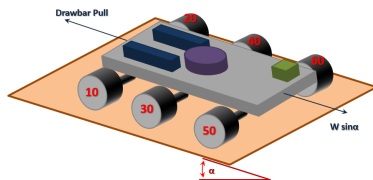


Figure 135: Rover ascending a slope.

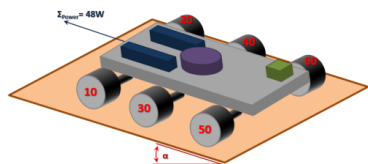


Figure 146: Rover ascending, consumption is 48W.

In other terms, using a database of traction and energetics – related experimental results for a specific wheel design, we can expect a fair approximation of the traction behaviour of a rover with known geometry and similar wheels, operating at similar soil conditions. In a parallel way, disposing of a large number of experimental results from a wheel actuator, provides a fair indication of the energetics of a similar actuator operating the wheels of the simulated rover mentioned above under the same conditions.

On the basis of this principle, we have incorporated a great number of traction and energetics – related experimental results from AWE wheels, as well as results related to AWE actuator energetics into the 3DROCS environment, enhancing its capacity to apply these results to any rover design, (using similar wheels and actuators), and calculate its behaviour in terms of traction capacity and energetic, in the context of (for example) the SFR mission. Figures 15-16 show an example of such implementation.

The geometry of the rover is introduced in the simulation platform, including mass of the different components. The system then calculates the axis loads per wheel according to terrain conditions. The resulting axis load is re-introduced in the simulation, predicting the capacity of the rover to negotiate, for example a slope, if $\sum DB > W \sin \alpha$.

Using experimental results, traction and energetics per wheel are derived as a function of soil condition, slip ratio and calculated axis load. If the produced drawbar pull permits the negotiation of the slope, the simulation shows the rover climbing up. In other case, the rover remains on the same spot.

Similarly, the power needs of the rover for locomotion are also calculated, using the experimental results, on real time, at any point of its trajectory. By estimating the power needed at any moment by each wheel of the rover, the overall cost for a given trajectory is obtained, (for example going from A to B, as illustrated in the Fig. 17).

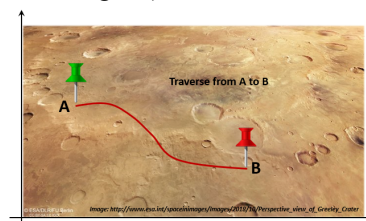


Figure 15: Traverse from A to B.

In that way, the efficiency can be derived and an optimal configuration in terms of speed or wheel stiffness, can be found.

7. Conclusions

This paper presents the results of AWE (ESA Contract Number 4000112936/14/NL/SFE) project, dealing with

adaptable wheels for planetary exploration rovers. The wheels provide the opportunity to perform many experiments, relating wheel stiffness, with traction and energetics on various soil conditions. The test results indicate that it is possible to optimize the wheel parameters, (such as stiffness), for optimal performance, (traction, energy spent), on various soil conditions. Taking also into account the wheel actuator, the tests appear to offer the possibility to predict the wheel behavior, (and the behavior of a rover utilizing these wheels), including the power and energy needed for given soil conditions. These results have been incorporated as an application example in the 3DROCS rover operations planning tool, presenting the capacity of the system to simulate an entire traverse, (in this case the SFR mission), and predict the estimated energy needs on the basis of the experimental data.

8. Bibliography

1. Bekker M.G. (1955). *Theory of Land Locomotion*. Ann Arbor. The University of Michigan Press.
3. Bekker M.G. (1963). *Mechanics of Locomotion and Lunar Surface Vehicle Concepts*. Defence Research Laboratories, General Motors Corp.
4. Wong J.Y. (2010). *Terramechanics and Off-road Vehicle Engineering*. Elsevier.
5. Wong, J.Y., et al. (1998) "Optimization of the Tractive Performance of Four-Wheel-Drive Tractors: Theoretical Analysis and Experimental Substantiation," *Proc. Inst. Mech. Eng. D J. Automob. Eng.*, vol. 212, no. 4.
6. Carrier, W.D.; Olhoeft, G.R.; and Mendell, W. (1991). *Physical Properties of the Lunar Surface. Lunar Sourcebook*, Grant H. Heiken, David T. Vaniman, and Bevan M. French, eds., Cambridge University Press, New York, NY.
7. Gill, W.R., Vanden B., Glenn E. (1968). "Soil Dynamics in Tillage and Traction." *U.S. Department of Agriculture*, Washington, DC.
8. Macdonald M., Badescu V. (2014). *The International Handbook of Space Technology*, Springer.
9. Siciliano B., Khatib O. (2008) *Springer Handbook of Robotics*, Springer.
10. Kobayashi T., Fujiwara Y., Yamakawa J., Yasufuku N., Omine K. (2010). "Mobility performance of a rigid wheel in low gravity environments." *Journal of Terramechanics*, 47 p.261-274.
11. Wong J.Y. (2012). "Predicting the performances of rigid rover wheels on extraterrestrial surfaces based on test results obtained on Earth." *Journal of Terramechanics*, 49 p.49-61.
12. Meirion-Griffith G., Nie C., Spenko M. (2014) "Development and experiment validation of an improved pressure-sinkage model for small-wheeled vehicles on dilative, deformable terrain." *Journal of Terramechanics*, 51 p.19-29.
13. Hambleton J.P., Drescher A. (2009). "Modelling-induced rutting in soils: Rolling." *Journal of Terramechanics*, 46 p.35-47.
14. Hambleton J.P., Drescher A. (2008). "Modelling-induced rutting in soils: Indentation." *Journal of Terramechanics*, 45 p.201-211.
15. Lyasko M. (2010). "LSA model for sinkage predictions." *Journal of Terramechanics*, 47 p.1-19.
16. Lyasko M. (2010). "Slip sinkage effect in soil-vehicle mechanics." *Journal of Terramechanics*, 47 p.21-31.
17. Laughery S., Gerhart G., Goetz R. Bekker's "Terramechanics model for off-road vehicle research." *US Army TARDEC Warren*, MI 48397-5000.
18. Ishigami G., Miwa A., Nagatani K., Yoshida K. (2007). "Terramechanics-based model for steering manoeuvre of planetary exploration rovers on loose soil." *Journal of Field Robotics* 24(3), 233-250.
19. Lee J.H., Gard K. (2014). "Vehicle-soil interaction: Testing, modelling, calibration and validation." *Journal of Terramechanics*, 52 p.9-21.
20. Asnani V., Delap D., Creager C. (2009). "The development of wheels for the Lunar Roving Vehicle." *Journal of Terramechanics*, 46 p.89-103.
21. Creager C. and Asnani V. (2017). "Drawbar Pull (DP) Procedures for Off-Road Vehicle Testing." *NASA/TP-2017-219384*.
22. Transcossi M. (2015). "What price of speed? A critical revision through constructal optimization of transport modes." *Int. J. Energy Environ Eng.*
23. Moreland S, Creager C., Padula S. (2018). "SFR Compliant Wheel Information for ESA." *NASA, JPL*.